NeuroImage 200 (2019) 199–209

Contents lists available at ScienceDirect

NeuroImage

journal homepage: www.elsevier.com/locate/neuroimage

MRI-based measures of intracortical myelin are sensitive to a history of TBI and are associated with functional connectivity

Evan M. Gordon [a,b,c,*], Geoffrey J. May [a,b,c,d], Steven M. Nelson [a,b,c,d]

[a] VISN 17 Center of Excellence for Research on Returning War Veterans, 4800 Memorial Dr, 151-C, Waco, TX, 76711, USA
[b] Center for Vital Longevity, School of Behavioral and Brain Sciences, University of Texas at Dallas, 1600 Viceroy Dr #800, Dallas, TX, 75235, USA
[c] Department of Psychology and Neuroscience, Baylor University, Baylor Sciences Building Suite B.309, Waco, TX, 76706, USA
[d] Department of Psychiatry and Behavioral Science, Texas A&M Health Science Center, College of Medicine, 8441 Riverside Parkway, Bryan, TX, 77807, USA

ARTICLE INFO

Keywords:
Traumatic brain injury
MRI
Biomarker
Intracortical myelin
Functional connectivity

ABSTRACT

Traumatic brain injuries (TBIs) induce persistent behavioral and cognitive deficits via diffuse axonal injury. Axonal injuries are often examined in vivo using diffusion MRI, which identifies damaged and demyelinated regions in deep white matter. However, TBI patients can exhibit impairment in the absence of diffusion-measured abnormalities, suggesting that axonal injury and demyelination may occur outside the deep white matter. Importantly, myelinated axons are also present within the cortex. Cortical myelination cannot be measured using diffusion imaging, but can be mapped in-vivo using the T1-w/T2-w ratio method. Here, we conducted the first work examining effects of TBI on intracortical myelin in living humans by applying myelin mapping to 46 US Military Veterans with a history of TBI. We observed that myelin maps could be created in TBI patients that matched known distributions of cortical myelin. After controlling for age and presence of blast injury, the number of lifetime TBIs was associated with reductions in the T1-w/T2-w ratio across the cortex, most significantly in a highly-myelinated lateral occipital region corresponding with the human MT+ complex. Further, the T1-w/T2-w ratio in this MT+ region predicted resting-state functional connectivity of that region. By contrast, a history of blast TBI did not affect the T1-w/T2-w ratio in either a diffuse or focal pattern. These findings suggest that intracortical myelin, as measured using the T1-w/T2-w ratio, may be a TBI biomarker that is anatomically complementary to diffusion MRI. Thus, myelin mapping could potentially be combined with diffusion imaging to improve MRI-based diagnostic tools for TBI.

1. Introduction

Traumatic brain injury (TBI) represents a significant medical burden both in the general population, where TBIs accounted for approximately 2.8 million emergency department visits, hospitalizations, and deaths in 2013 alone (Taylor et al., 2017), as well as in the U.S. military and Veteran population, where TBI is argued to be the signature wound of U.S. military personnel who fought in Iraq and Afghanistan (Wojcik et al., 2010). TBIs can result in deficits in learning and memory, anxiety and mood, and executive function (Agoston and Kamnaksh, 2015; Bruce, 2010; Cole and Bailie, 2016; Kennedy et al., 2010; Rosenfeld and Ford, 2010; Thompson et al., 2008; Ursano et al., 2010). While cognitive and behavioral deficits caused by "mild" TBI often (though not always) resolve without intervention (Belanger et al., 2005; Dikmen et al., 2001; Hessen et al., 2007), deficits caused by more severe TBIs may persist for years or throughout the patient's lifetime (Langlois et al., 2006; Vanderploeg et al., 2007, 2009; Zaloshnja et al., 2008).

In principle, an accurate diagnosis of TBI severity could be highly useful in predicting a patient's expected level of long-term deficit and in gaining access to rehabilitative services. However, assessments of TBI are usually not based on any neurobiological measure, but are made based on the severity of post-TBI symptoms, including the presence and duration of consciousness loss immediately after the injury, the presence of altered consciousness, and the presence of post-TBI amnesia (Corrigan and Bogner, 2007; Vasterling et al., 2008). Perhaps as a result, post-TBI symptom-based assessments are only weakly predictive of behavioral outcomes, usually accounting for less than 10% of the variance in cognitive function or quality of everyday life (Cappa et al., 2011; Chien et al., 2017; Hiekkanen et al., 2009; Rohling and Demakis, 2010). Thus, there is a significant need for more advanced diagnostic techniques that can effectively measure the impacts that TBIs have on the brain in order

* Corresponding author. VISN 17 Center of Excellence for Research on Returning War Veterans, 4800 Memorial Dr, 151-C, Waco, TX, 76711, USA.
E-mail address: evan.gordon@va.gov (E.M. Gordon).

https://doi.org/10.1016/j.neuroimage.2019.06.026
Received 5 April 2019; Received in revised form 29 May 2019; Accepted 12 June 2019
Available online 13 June 2019
1053-8119/Published by Elsevier Inc.

Abbreviations

TBI	traumatic brain injury
MRI	magnetic resonance imaging
fMRI	functional magnetic resonance imaging
LoC	loss of consciousness
PTA	post-traumatic amnesia
TE	echo time
TR	time of repetition

to deliver accurate prognoses.

In the most common case of a closed-head injury, TBI-related cognitive dysfunction is believed to be driven by the presence of diffuse axonal injury (Pearce, 2008; Silver et al., 2011). In this type of injury, the axonal projections that connect brain regions are severed and/or demyelinated by shearing forces induced by a head impact or blast wave. This axonal damage in turn is believed to impair networked brain communication, resulting in cognitive impairment (Hayes et al., 2016; Kaplan et al., 2018). These effects on myelinated axonal processes have led to extensive scientific interest in examining TBI-related reductions in the integrity of large white-matter tracts. Such investigations typically use diffusion MRI techniques that detect variations in the anisotropic diffusion of water to identify disruption in white matter regions. This extensive corpus of work broadly indicates white matter abnormalities in TBI (see e.g. Huisman et al., 2004; Kraus et al., 2007; Mac Donald et al., 2011; Rutgers et al., 2008a, 2008b; Wozniak et al., 2007; for more comprehensive reviews, see Asken et al., 2018; Douglas et al., 2015; Fox et al., 2013; Hulkower et al., 2013; Kaplan et al., 2018; Niogi and Mukherjee, 2010; Sharp and Ham, 2011; Shenton et al., 2012; Strauss et al., 2015), though the particular locations of disruption vary substantially from study to study and individual to individual, suggesting that TBI-induced white matter abnormalities are spatially heterogeneous (Davenport et al., 2012; Hayes et al., 2015; Jorge et al., 2012; Mac Donald et al., 2011; Taber et al., 2015; Wallace et al., 2018a; Ware et al., 2017). Diffusion-related measures of white matter integrity have also been consistently correlated with TBI outcomes such as clinical symptoms and cognitive function (e.g. Gordon et al., 2018; Gu et al., 2013; Kraus et al., 2007; Kumar et al., 2009; Matsushita et al., 2011; Palacios et al., 2011; Wada et al., 2012; Xiong et al., 2014; see also meta-analyses by van Eijck et al., 2018; Roberts et al., 2016; Wallace et al., 2018b).

While diffusion-related measures of white matter myelination have been of high scientific interest in TBI due to their ability to differentiate TBI groups from healthy controls and their association with outcomes, they have not successfully been linked to disruptions in networked brain communication. We previously demonstrated that diffusion measures of white matter myelination were affected by TBI, but were uncorrelated with TBI-influenced fMRI measures of brain communication (Gordon et al., 2018). Perhaps as a result, diffusion measures have not been successfully used for TBI diagnosis. For example, Mac Donald et al. (2011) used diffusion imaging to identify statistically robust TBI-related white matter abnormalities, both diffusely and in multiple focal regions. However, they critically noted that many TBI patients did not have detectable diffusion imaging abnormalities in the white matter, and they concluded that diffusion scans could not be used in place of a clinical, symptom-based diagnosis. Based on findings such as these, Douglas et al. (2015) recently argued that current diffusion techniques are only sensitive to differences at the group level, and have not yet demonstrated clinical utility at the individual level. While diffusion images clearly carry some useful information about TBI, the fact that 1) TBI in some individuals can occur without diffusion abnormalities, and 2) diffusion effects do not explain TBI-related influences on brain communication, suggests that in at least some individuals, TBI-related injuries that affect brain function may occur outside the deep white matter structures that are the primary focus of diffusion scans.

The loss of axonal myelin sheathing may be a major contributing factor to TBI-related disruptions in white matter integrity and resulting symptoms (Shi et al., 2015). Importantly, this myelin sheathing is not present only in the deep white matter. Rather, it extends into the cortical mantle itself, where initial and terminal processes of large pyramidal cells, as well as short-range axonal processes of cortical interneurons, are often heavily myelinated (Nieuwenhuys, 2013). Such intracortical myelination has been the basis of a great deal of study, most notably inspiring the subfield of myeloarchitectonics as an alternative (Hopf, 1951) or complement (e.g., Palomero-Gallagher and Zilles, 2017) to the study of the cytoarchitectonic organization of the brain. TBIs, which are argued to affect cognition and behavior via the damage and demyelination of long-range axons, could also plausibly reduce intracortical myelination. If true, intracortical myelin could serve as a diagnostic biomarker for TBI that, in being localized to cortex, better relates to cortical function, and so is complementary to measures of deep white matter myelination.

Unfortunately, the integrity of these myelinated intracortical axons is difficult to measure using standard diffusion imaging, as the myelinated axons in cortex are not as dense or as consistently aligned as they are in subcortical white matter tracts. While multiple works have demonstrated some ability characterize axonal orientations in cortex using very high-resolution diffusion imaging (Heidemann et al., 2012; McNab et al., 2013; Song et al., 2014) or novel analysis techniques (Rathi et al., 2014), it is unclear to what extent these techniques can actually assess axonal integrity or myelination within the cortex.

Importantly, in 2011, Glasser and Van Essen introduced a noninvasive MRI-based technique to map the density of intracortical myelin in the human brain. This technique emerged from the realization that both T1-weighted (Sigalovsky et al., 2006) and T2-weighted (Yoshiura et al., 2000) MRI images are partially sensitive to cortical myelin content, but in different directions; and thus, that calculating the ratio between the T1-w and T2-w image could dramatically improve myelin-related contrast. This myelin mapping technique, which has been shown to converge with histologically-derived maps of cortical myelin (Nieuwenhuys and Broere, 2017), has illustrated the distribution of intracortical myelin across the cortex in living humans (Ganzetti et al., 2014; Glasser and Van Essen, 2011; Glasser et al., 2016; Shafee et al., 2015), and has been used to parcellate the cortex into cortical areas (Glasser et al., 2016). It has also been used to show that intracortical myelin 1) is affected by aging and associated with cognitive performance (Grydeland et al., 2013); 2) is associated with individual differences in fMRI- (Gordon et al., 2017a) and EEG-derived (Grydeland et al., 2016) measures of cortical function; and 3) is reduced in multiple sclerosis (Righart et al., 2017) and schizophrenia (Iwatani et al., 2015). Together, this work suggests that the myelin mapping technique provides information that is relevant for brain organization and cortical function, and is sensitive to disease states. However, this approach has not previously been explored as a potential biomarker for TBI-related damage.

Here, we explored whether measures of intracortical myelin are sensitive to the number of lifetime TBIs by employing the T1-w/T2-w myelin mapping technique in 46 U.S. military Veterans with a history of TBI. Because TBI-related reductions in axonal integrity have previously been described as occurring both strongly in specific focal regions and diffusely across the brain (Davenport et al., 2012; Jorge et al., 2012; Mac Donald et al., 2011), we tested for effects of TBI on cortical myelin both in specific focal cortical regions and diffusely across the cortex. Further, because exposure to a blast has been argued to alter white matter integrity through different mechanisms than blunt-force impact (Bass et al., 2012; Davenport et al., 2012; Ganpule et al., 2013; Taber et al., 2015), we tested whether a history of blast-induced TBI alters cortical myelin content above and beyond the number of TBIs. Finally, we collected resting-state fMRI in a subset of patients in order to test whether TBI-influenced intracortical myelin is associated with the strength of networked brain communication.

2. Materials and methods

2.1. Participants

Data were collected from US Military Veterans with a self-reported history of TBI recruited from the areas surrounding Waco, TX. Participants were carefully selected as a subset of 62 individuals from three separate studies who exhibited the highest quality MRI images (see "Quality control of MR images", below). The final sample included 46 Veterans (40M, 6F).

Before beginning their study participation, participants were screened and excluded for MRI safety issues, any Axis I psychotic disorder, bipolar disorder, dementia, substance abuse disorder, or any substance use in the last 12 h before MRI scanning. Written informed consent was obtained from all participants. All studies included in this work were approved by the Central Texas Veterans Health Care System Institutional Review Board.

2.2. TBI assessment

We used self-report measures to determine each individual's history of TBI. We principally assessed the number of TBI events using an established rubric: any event with loss of consciousness OR a dazed feeling OR post-traumatic amnesia was rated as a TBI. Additionally, we assessed the cause of each TBI event in order to determine whether each participant had any history of blast-related TBI (which did not preclude a history of impact TBI). Additional information collected included the severity of the TBI, the length of any loss of consciousness (LoC), and the presence of post-traumatic amnesia (PTA). These assessments were conducted using the Vasterling TBI assessment interview (Vasterling et al., 2008) (19 participants) and the Ohio State University TBI Identification Method (Corrigan and Bogner, 2007) (27 participants); these two screening tools vary in details, but they both assess all information needed to determine the number of lifetime TBIs and cause of each TBI, as described above.

2.3. MRI image acquisition

Imaging was performed on a Philips Achieva 3T MRI scanner. The anatomical scanning session included collection of one T1-weighted turbo field echo image and one T2-weighted multislice turbo spin-echo image. Scanning parameters were as follows: T1-weighted sagittal image —TE = 3.08 ms, TR partition = 2.4 s, TI = 1000 ms, flip angle = 8°, 176 slices, 1 × 1x1 mm voxels; T2-weighted sagittal image—TE = 80 ms, TR partition = 3s, flip angle = 90°, 161 slices, 1 × 1x1 mm voxels.

32 participants additionally underwent between one and five two-hour sessions of resting-state fMRI scanning, during which they were instructed to remain awake, stay as still as possible, and fixate on a white crosshair. These sessions were conducted on separate days spanning less than three months from the anatomical acquisitions. Across all sessions, participants were scanned for multiple gradient-echo echo-planar imaging runs, with each run lasting 6 min 36 s and having the following parameters: TE = 30 ms, flip angle = 90°, in-plane resolution = 3 × 3 mm, 34 3.0 mm-thick axial slices with a 1.0 mm gap between slices, TR = 3.0s, 132 vol acquired per run. The minimum number of these scanning runs acquired across participants was 6 (~40 min) and the maximum number of runs scanned was 45 (297 min). At the beginning of each scanning session, a double-echo gradient echo field map image was collected with ΔTE = 2 ms and with the same dimensionality as the fMRI images.

2.4. Quality control of structural MR images

Participant motion during T1-w and T2-w scanning can introduce artifacts into the images which may reduce the quality of cortical segmentations, as well as corrupt measures based on relative MR image intensities. Thus, all images were visually screened for any evidence of motion in three orthogonal views by an expert rater. Screening particularly focused on identifying the presence of typical motion-induced "ringing" artifacts, as well as the presence of shifts in brain position from one sagittal slice to the next. Any participant exhibiting either of these effects in either the T1-w or T2-w image was excluded from further analysis. We also closely examined the images for the presence of cortical lesions, and we excluded one participant on this basis. Finally, we assessed the quality of the T1-w-to-T2-w registration, which is critical for calculating the myelin-sensitive T1-w/T2-w ratio; one participant was excluded for having poor registration. In total, forty-six participants were found to have artifact-free T1-w and T2-w images and good T1-w-to-T2-w registration and were included in the final study.

In screening for motion-related effects, we found that two participants exhibited a highly localized signal dropout in the frontal pole of their T2-w image. Because the quality of the rest of the scans was high in these participants, we elected to retain these participants and exclude data from these participants in this small region (which is not an area of high cortical myelin content (Glasser and Van Essen, 2011)) from all analyses.

2.5. Myelin mapping analysis procedures

Procedures for mapping the myelin content of the cortical surface followed (Glasser and Van Essen, 2011); see Fig. 1A for an illustration of the concept.

First, cortical surfaces were generated from each participant's T1-weighted image, following procedures described in (Glasser et al., 2013). Specifically, anatomical surfaces were generated from the participant's T1-weighted image using FreeSurfer's default recon-all processing pipeline (version 6.0). This pipeline included brain extraction, segmentation, generation of white matter and pial surfaces, inflation of the surfaces to a sphere, and surface shape-based spherical registration of the subject's 'native' surface to the fsaverage surface (Dale and Sereno, 1993; Dale et al., 1999; Fischl et al., 1999; Ségonne et al., 2004, 2005). The fsaverage-registered left and right hemisphere surfaces were then brought into register with each other (Van Essen et al., 2012) and resampled to a resolution of 164,000 vertices using Caret tools (Van Essen et al., 2001). Finally, each subject's surface was down-sampled to a 32,492 vertex surface (fs_LR 32k), which allowed for analysis in a computationally tractable space. The above procedure results in a surface space that allows for quantitative analysis across subjects. A script for this procedure is available on the Van Essen Lab website (Freesurfer_to_fs_LR Pipeline, http://brainvis.wustl.edu/wiki/index.php/Caret:Operations/Freesurfer_to_fs_LR).

Subsequently, the T1-weighted image was brain-extracted and segmented into white matter and cerebro-spinal fluid using the FAST procedure (Zhang et al., 2001) implemented in FSL (Jenkinson et al., 2012). The T2-weighted image was brought into register with the T1-w image by calculating a linear warp via the boundary-based registration method in FSL (Greve and Fischl, 2009), using the FAST-derived gray--white boundary. To facilitate comparisons of T1-w and T2 images across participants scanned on different days, both the T1-w and aligned T2 images were then normalized by dividing the image by the average value of each image within the FAST-derived cerebro-spinal fluid segmentation. At each voxel, the ratio between the normalized T1-w image and the aligned normalized T2 image was calculated. Within the cortical ribbon, this ratio is believed to be contrast-sensitive to myelin and so is argued to be related to myelin density (Glasser and Van Essen, 2011) (see Fig. 1A).

To specifically examine only cortical voxels, this T1-w/T2 ratio image was sampled to the cortical surface using the following steps. First, the cortical ribbon was defined as all voxels between the white and pial surfaces. Subsequently, the T1-w/T2 ratio volumes were sampled to each subject's individual 'native' midthickness surface (generated as the average of the white and pial surfaces). This was done by employing the ribbon-constrained volume-to-surface sampling procedure available in Connectome Workbench 1.2 (Marcus et al., 2011), which samples data

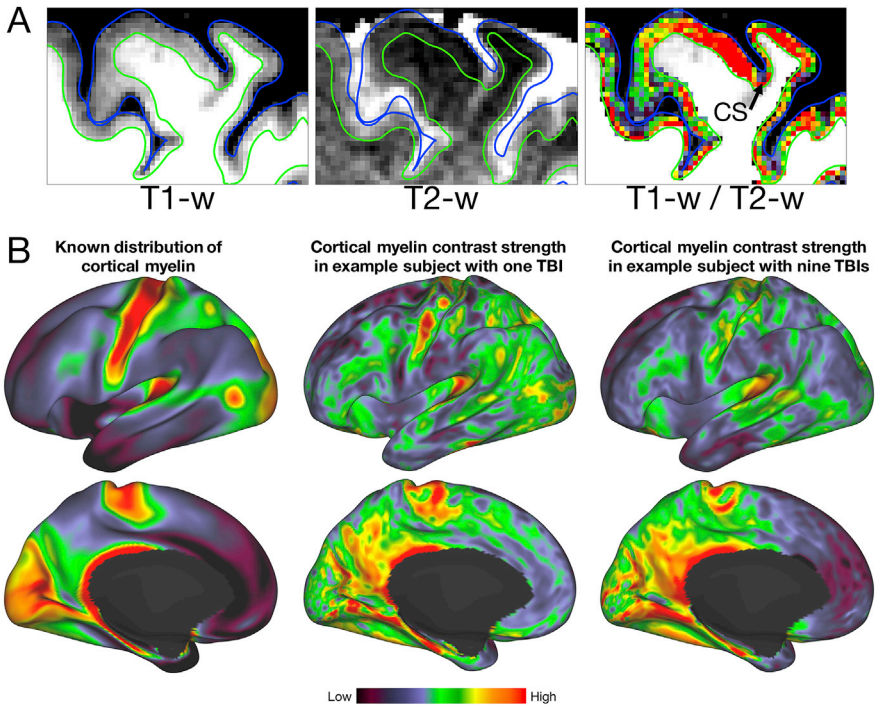

Fig. 1. Mapping intracortical myelin in the human brain. A) Illustration of the procedure for mapping intracortical myelin (Glasser and Van Essen, 2011). A T1-weighted (left) and T2-weighted (middle) image were registered to each other, and a ratio between the two images was calculated in each voxel (right), representing myelin content. Values between the pial surface (blue lines) and the gray-white border (green lines) represent intracortical myelin in the region surrounding the central sulcus (marked "CS"), and were mapped onto a 2D cortical surface. B) Distribution of the intracortical myelin contrast signal across the brain. The spatial distribution of the cortical myelin contrast calculated across 210 healthy controls (in Glasser et al., 2016; data available at https://balsa.wustl.edu/mpwM) was similar to those observed in individual subjects with few (middle) and with many (right) lifetime TBIs.

from voxels within the cortical matter ribbon, and using the "myelin--style" option (Glasser and Van Essen, 2011). The myelin-style sampling procedure enabled us to 1) exclude from the sampling all voxels with T1-w/T2 ratio values greater than 2 standard deviations from the mean ratio value across all cortical voxels; 2) regress out confounding effects of cortical thickness (as calculated by Freesurfer); and 3) conduct sampling weighted by a spatial Gaussian kernel with $\sigma = 1.7$.

Once sampled to the 'native' surface, T1-w/T2 ratio images were deformed and resampled from the individual's 'native' surface to the 32k fs_LR surface, and data from the two hemispheres were combined into the CIFTI format. The ratio images were smoothed along the 32k fs_LR surface using a Gaussian smoothing kernel ($\sigma = 1.7$). These T1-w/T2 ratio maps represent intracortical myelin content at each vertex on the cortical surface (Glasser and Van Essen, 2011).

2.6. Association between intracortical myelin content and TBI

At each cortical vertex, we conducted partial correlations of the strength of the myelin contrast against the number of lifetime TBIs reported. In these partial correlations, we also controlled for effects of 1) a history of blast-related TBI, and 2) participant age as effects of no interest. This was done both because of the known effects of age on the strength of intracortical myelin contrast (Grydeland et al., 2013), and because these three factors—age, number of lifetime TBIs, and a history of blast TBI—were all found to be associated with each other (see Results). To further determine whether any other factors might be driving these effects, we repeated this analysis multiple times after regressing out effects of participant sex, presence of PTA after the worst lifetime TBI, time since the most recent TBI, severity of the worst lifetime TBI, and length of LoC after the worst lifetime TBI. In these analyses, sex, presence of PTA, and severity of worst TBI were treated as categorical variables, while time since most recent TBI and length of LoC after worst lifetime TBI were treated as continuous variables.

We hypothesized that TBIs would reduce the intracortical myelin contrast in a broad, diffuse manner, which would manifest as a consistent, widespread negative association between TBI and myelin content across much of the cortex. We thus examined the distribution of average partial R values resulting from the TBI-myelin correlation across the cortex in order to determine whether the distributions of these values were centered away from zero. A non-zero centering of this distribution would indicate broad TBI-myelin effects across many cortical vertices. To determine the significance of any observed non-zero centering, we used a permutation-based null, in which participant labels were randomly permuted across 10,000 iterations to create many "null" partial correlation maps. In each iteration, we calculated the mean partial R value across the cortex. The significance of the non-zero centering of the real distributions were then calculated as the proportion of null iterations with mean partial R values more negative than the real distribution.

We also tested whether the strength of intracortical myelin contrast was significantly related to TBI in any specific cortical regions. To establish a significance threshold, we corrected the partial correlation map for multiple comparisons by again employing a permutation-based cluster correction, in which participant labels were randomly permuted across 10,000 iterations to create many "null" partial correlation maps. Together, these null maps generate a null distribution of variously-sized surface clusters of high correlation that occur by chance. Clusters of significant vertices observed in the real data were then evaluated to determine how often "significant" clusters of the same or larger size were observed in the null maps. This permutation-based correction avoids many of the assumptions about spatial autocorrelations in MRI data made by other cluster correction approaches based on 3D Gaussian random field theory, which not only have been shown to inflate false positive rates (Eklund et al., 2016), but which also are likely invalid in surface-based analyses (as surface-mapped data is not smooth in 3D Euclidean space, but rather on the convoluted 2D surface). This approach is similar to the surface-based cluster correction procedure employed by (Gordon et al., 2017b).

2.7. Effect of blast TBI on intracortical myelin content

Blast-related TBI has been argued to have a distinct impact on axonal myelination compared to TBI resulting from a blunt-force impact (Bass et al., 2012; Ganpule et al., 2013). Therefore, we assessed the effect of blast-related TBI on the strength of the intracortical myelin contrast. At

each cortical vertex, we conducted a two-sample *t*-test to determine whether residual myelin contrast was higher in participants with a history of non-blast TBI than those with blast TBI. This *t*-test was conducted after regressing out the effects of number of TBIs and of age from the myelin values. As above, we also examined the distributions of the resulting t-scores to determine whether they were significantly shifted from zero, which would indicate a broad and diffuse effect of blast, with statistical significance again determined using a permutation-based null model. Vertex-wise correction for multiple comparisons were again conducted via permutation-based cluster correction.

2.8. FMRI processing

Functional data were preprocessed using FSL tools and in-house Matlab scripts. For each field map acquisition, the field map image was calculated. Each fMRI run then underwent within-run correction for head movement, and the field map magnitude image was linearly registered to the run's motion-corrected temporal average. This registered field map image was used to correct for distortion in the fMRI run. All un-distorted runs were then registered to each other, and the cross-run average fMRI image was computed. A linear warp was then calculated from the cross-run fMRI image to the native T1-w image using the boundary-based registration method (Greve and Fischl, 2009). The across-run, average run-to-T1-w, and T1-w-to-MNI transformations were concatenated with an interpolation into 3-mm isotropic space and applied to each un-distorted run. The resulting MNI-space fMRI runs were intensity-normalized to a whole brain mode value of 1000.

Additional preprocessing steps to reduce spurious variance were executed as recommended in (Ciric et al., 2017; Power et al., 2014). First, motion parameters were temporally filtered to eliminate spurious head motion caused by breathing-related chest movement influences on the B0 magnetic field (following Fair et al., 2018). Temporal masks were then created to flag and censor motion-contaminated frames. Motion contaminated volumes were identified by frame-by-frame displacement (FD, described in (Power et al., 2012)). Frames with filtered FD > .2 mm were flagged as motion-contaminated. Two participants were found to have less than thirty minutes of motion-free data and were excluded from further fMRI analysis, leaving a final sample size of 30 participants with fMRI data. The remaining participants retained on average 67.8% ± 28.6% of collected data, constituting 139.3 ± 83.7 min of data.

After computing these temporal masks, data were processed with the following steps: (i) demeaning and detrending; (ii) concatenation across runs; (iii), multiple regression of nuisance signals including: top principal components explaining large portions of the variance in whole brain signals, white matter signals, and ventricular signals (Marek et al., 2018); run identity; session identity; and motion regressors derived by Volterra expansion (Friston et al., 1996), with censored data ignored during beta estimation; (iv) interpolation across censored frames (Carp, 2013; Power et al., 2012); and (v) band-pass filtering (0.009 Hz < f < 0.08 Hz). Censored frames were then excised for all subsequent analyses.

The fMRI volumetric timeseries were then sampled to each subject's left and right-hemisphere cortical surfaces using the ribbon-constrained sampling procedure (Glasser and Van Essen, 2011) in Connectome Workbench 1.0 (Glasser et al., 2013). Surface-space timecourses were deformed and resampled to the 32k fs_LR surface. Finally, the resting-state timecourses were smoothed with geodesic 2D Gaussian kernels (FWHM = 6 mm).

2.9. Association between intracortical myelin and resting-state functional connectivity

To preview results from the above analyses, we identified a region in left lateral occipital cortex in which the strength of the intracortical myelin contrast was reduced by a greater number of lifetime TBIs. To determine whether this myelin reduction was associated with alterations in functional connectivity, we employed a previously-published parcellation of human cortex (Gordon et al., 2016). We found that the TBI-influenced region aligned closely with a single a priori parcel in the Visual network. We hypothesized that if reduced myelin affects the strength of functional connectivity, it will likely reduce the strong within-network connections, which are believed to most represent networked area-to-area brain communication. Thus, for each participant with fMRI data we calculated the strength of functional connectivity between this myelin-influenced region and the rest of the Visual network. This was calculated as the correlation between the average fMRI timecourse within the region and the average fMRI timecourse across all Visual network parcels. We then Fisher-transformed this connectivity strength to improve normality. Finally, we correlated the average intracortical myelin contrast value within the affected region against this Visual network connectivity strength across participants.

2.10. Data and code availability statement

All analysis code will be made available upon direct request.

Data cannot be made publicly available in order to comply with the requirements of the US Department of Veterans Affairs and the Central Texas Veterans Health Care System (CTVHCS) Institutional Review Board. Data can be made available upon direct request after establishing a formal Memorandum of Understanding with the authors through the CTVHCS IRB.

3. Results

3.1. Participant characteristics

The forty-six participants retained for the final analysis had an average age of 37.4 ± 9.8 years. On average, these participants had experienced 3.2 ± 2.1 lifetime TBIs (range: 1–9). The average amount of time that had passed since the most recent TBI was 9.0 ± 9.6 years (range: 3 months–41 years).

In characterizing the worst lifetime TBI, we found that 35 participants had experienced only mild TBIs; 8 had experienced at least one Moderate TBI; and 3 had experienced at least one Severe TBI. For this worst lifetime TBI, 14 participants experienced no loss of consciousness (LoC); 2 experienced LoC of less than one minute; 21 experienced LoC between one and thirty minutes; 7 experienced LoC between thirty minutes and 24 h; and two experienced LoC longer than 24 h 29 participants reported at least some post-traumatic amnesia (PTA) from their worst TBI, while 10 reported no PTA (and 7 did not respond to this question).

Participant age was weakly but nonsignificantly correlated with the number of lifetime TBIs ($r = -0.27$, $p = .074$). Of these 46 participants, 28 reported at least one blast-related TBI. Participants with a history of blast-related TBI tended to be younger ($t(44) = -2.55$, $p = .014$) and to have experienced more total TBIs ($t(44) = 3.13$, $p = .003$) than those with no history of blast-related TBI.

3.2. Intracortical myelin content can be mapped in individual participants with and without TBI

In each participant, the cortical myelin mapping procedure successfully produced maps that resemble the known spatial distribution of cortical myelin across many healthy controls (Glasser and Van Essen, 2011; Glasser et al., 2016). Fig. 1B shows this canonical myelin distribution (left), as well as myelin maps from two example participants with one (middle) and with nine (right) TBIs. In the canonical map and in each participant, the myelin contrast was most highly elevated in primary sensory and motor areas (i.e. central sulcus, posterior insula/superior temporal gyrus, medial occipital cortex), as well as in classic localized "hot spots" such as the posterior cingulate, medial temporal lobe, and the putative human MT+ area in lateral occipital cortex. These regions closely match areas shown to have high cortical myelin content in histological studies (Nieuwenhuys and Broere, 2017). In the canonical map

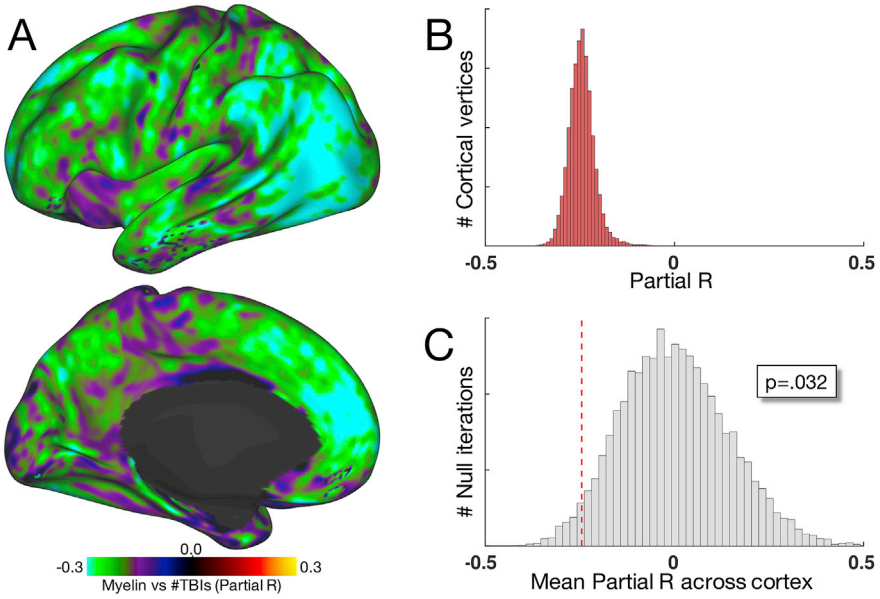

Fig. 2. Increasing number of lifetime TBIs is broadly associated with reduced intracortical myelin. A) Partial correlations between number of lifetime TBIs suffered and the intracortical myelin contrast signal (controlling for age and blast exposure) conducted at each cortical vertex. Note the consistent and widespread negative associations between the variables. B) The distribution of the strength of TBI-myelin associations. The vast majority of these partial R values are negative. C) The distribution of median partial R values after 10,000 random permutations of subject identity. The real median partial R value (red dotted line) was significantly more negative than the permuted values.

and across participants, more moderate myelin content was consistently observed in inferior parietal lobule and superior occipital cortex, as well as in posterior superior temporal sulcus. We conclude that the procedures previously employed to map intracortical myelin content in healthy controls (Glasser and Van Essen, 2011; Glasser et al., 2016; Gordon et al., 2017a) can be employed to produce similarly distributed maps in participants with a history of TBI.

3.3. A greater number of lifetime TBI events is broadly associated with lower cortical myelin

At each cortical vertex, we examined how the number of lifetime TBIs was associated with the strength of the intracortical myelin contrast. We found that effectively the entire cortex (99.96% of vertices) exhibited at least some negative association between the cortical myelin contrast and the number of lifetime TBIs (Fig. 2A). On average, cortical vertices were correlated with TBI number at partial $r = -0.245$, and the bulk of these associations (92.0%) were partial $r < -0.2$ or stronger (Fig. 2B).

Using a permutation-based null model, we tested whether the distribution of these TBI number – myelin associations was more negative than would be expected by chance. We observed that the mean of the cortical distribution of partial r values (partial $r = -0.245$) was more negative than 96.8% of the means of the null model cortical distributions, yielding a significant p value of .032 (Fig. 2C).

Effects of TBI number on myelin were not driven by participant sex, presence of PTA after the worst lifetime TBI, time since the most recent TBI, or severity of the worst lifetime TBI, as repeating this analysis after additionally regressing out each of these factors in turn also produced maps with widespread negative associations and almost identical spatial distributions (Figs. S1B,C,D,E). Interestingly, the magnitudes of the TBI number-myelin relationships were somewhat reduced after controlling for the length of LoC after the worst lifetime TBI, though the effects remained widely negative and still had a similar spatial distribution (Fig. S1F). This suggests that injuries resulting in extended LoC may also partially influence myelin. However, we also note that LoC of the worst TBI was correlated with the number of lifetime TBIs ($r(44) = 0.39$, $p = .013$); this is to be expected, as a greater number of TBIs will increase the chances of experiencing at least one TBI with extended LoC. Because these two factors are covariant, it is difficult to fully disentangle the effects of these factors in the present work.

3.4. A greater number of lifetime TBI events is specifically associated with lower cortical myelin in the human MT+ complex

We tested whether the widespread relationships between the number of TBI events and the strength of the cortical myelin contrast was significant in any specific region of the brain. A stringent permutation-based cluster correction approach established that for an overall corrected $p < .05$, the correction threshold was partial $r < -0.32$ (corresponding to $p < .01$ uncorrected) combined with a cluster extent threshold of 93.8 mm^2.

One cortical cluster survived this threshold in left lateral occipital cortex (Fig. 3A), indicating a particularly consistent relationship between the number of lifetime TBIs and cortical myelin in this region. A similar effect was also observed in the right hemisphere, but this cluster did not survive cluster correction.

Notably, this significant cluster overlapped very well with the average location across healthy subjects of the punctate, highly myelinated area in lateral occipital cortex believed to be the human MT+ complex (Glasser and Van Essen, 2011; see Fig. 3B).

3.5. Blast TBI does not significantly affect intracortical myelin

At each cortical vertex, we examined whether a history of blast TBI was associated with the strength of the intracortical myelin contrast, after controlling for age and number of lifetime TBIs. We found that subjects with a history of blast TBI had numerically greater intracortical myelin across most regions of cortex (Fig. S2A). However, the average t-score across the brain was only 0.51, which was not significantly different from the distribution of an iterated set of permuted null model brain maps ($p = .33$; Fig. S2B). Further, the effect was generally weak, with only 0.05% of cortex exhibiting t-scores greater than 1.69 (corresponding to $p < .05$ uncorrected), and no region surviving cluster-based correction for multiple comparisons (using a threshold of $t = 2.44$, corresponding to $p < .01$ uncorrected). As this the effect of blast was neither in the hypothesized direction nor significant, we cannot conclude that a history of blast TBI has an effect on intracortical myelin.

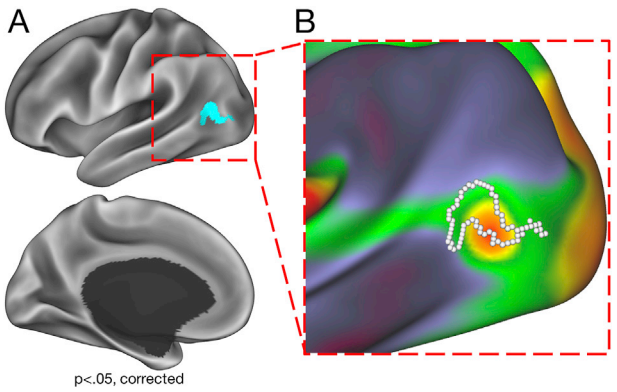

Fig. 3. Significant local associations between number of lifetime TBIs and intracortical myelin emerged most strongly in a region overlapping the human MT+ complex. A) The strength of the intracortical myelin contrast in a cluster in left lateral occipital cortex was significantly associated with number of lifetime TBIs (after controlling for age and blast exposure) after correcting for multiple comparisons. B) This significant cluster (outline in white dots) closely overlapped a myelin hotspot present across 210 healthy controls (in Glasser et al., 2016; data available at https://balsa.wustl.edu/mpwM), which was identified as the human MT+ complex by Glasser and Van Essen (2011).

3.6. Intracortical myelin in the left human MT+ complex is associated with the strength of functional connectivity between this region and the rest of the visual network

Intracortical myelin was most associated with TBI in a putative MT+ region (Fig. 3), a known visual processing region (Born and Bradley, 2005; Dubner and Zeki, 1971). Indeed, this region closely overlapped with a single a priori parcel within the Visual network (Fig. 4A). We observed that greater intracortical myelin in this MT+ region predicted stronger functional connectivity between this MT+ region and the rest of the Visual network ($r(29) = 0.49$, $p = .006$; Fig. 4B), suggesting that region-specific TBI-related reductions in intracortical myelin may affect that region's function. Post-hoc tests established that this effect was specific to the Visual network, as MT+ myelin was not associated with functional connectivity between the MT+ region and any of the other 11 brain networks described by (Gordon et al., 2016) (all $rs(29)<0.25$, all $ps > .18$).

4. Discussion

In this work, we conducted the first examination of how TBI affects intracortical myelin in the human brain. We found that suffering an increasing number of lifetime TBIs broadly and diffusely reduced the strength of the myelin-sensitive contrast within the cortex. We also found a specific region in lateral occipital cortex that exhibited TBI-related reductions in the intracortical myelin contrast, which were associated with lower functional connectivity. Together, these results suggest that the intracortical myelin contrast may serve as a potential biomarker of TBI-related brain damage and TBI influences on brain function.

Previous work has extensively investigated the effects of TBI on deep white matter integrity using diffusion imaging, and has consistently found that TBIs cause damage to these structures (Asken et al., 2018; Douglas et al., 2015; Fox et al., 2013; Hulkower et al., 2013; Kaplan et al., 2018; Niogi and Mukherjee, 2010; Sharp and Ham, 2011; Strauss et al., 2015). It is highly plausible that such damage may also extend to the myelinated axons found in the cortical mantle. While a non-invasive technique for mapping in-vivo intracortical myelin was introduced by (Glasser and Van Essen, 2011), since then it has been utilized only sparingly to examine effects of disease states on intracortical myelin (Iwatani et al., 2015; Righart et al., 2017), and it has never previously been used to test for effects of TBI. This spare usage of such a potentially powerful technique may be due to the substantial technical hurdles involved, particularly including the mapping of 3D volumetric data to the 2D cortical surface, as well as the challenge of conducting statistical tests on the 2D surface.

In overcoming these technical hurdles, we found that reductions in intracortical myelin associated with TBI are present across the cortex in a highly distributed fashion, and that these widespread effects on myelin were significant in a permutation test. This finding converges with previous reports of widespread closed-head TBI-related effects in diffusion imaging-derived estimates of white matter integrity (Davenport et al., 2012; Hayes et al., 2015; Jorge et al., 2012; Taber et al., 2015) and in functional MRI-derived estimates of brain connectivity (Bharath et al., 2015; Stevens et al., 2012; Vakhtin et al., 2013).

The mechanism by which TBIs reduce intracortical myelin are likely the same as those proposed to affect the deep white structures imaged by diffusion studies: namely, diffuse axonal injuries induced by stretching and deformation of brain tissue, which can result from the shearing forces induced by sharp acceleration/deceleration in a head impact (Davceva et al., 2012; Zhang et al., 2006) or from a blast pressure wave traveling through the brain (Bass et al., 2012; Elsayed, 1997; Ganpule et al., 2013; Moore and Jaffee, 2010). However, unlike diffusion measures of deep white matter injuries, the myelin contrast signal probably indexes damage not only to the long-range pyramidal cells that project into the deep white matter, but also to the short-range interneurons that are myelinated to varying degrees across the cortex (Nieuwenhuys, 2013). Thus, in characterizing TBI-related damage to cortical myelin, the myelin mapping technique can potentially identify interneuron-specific

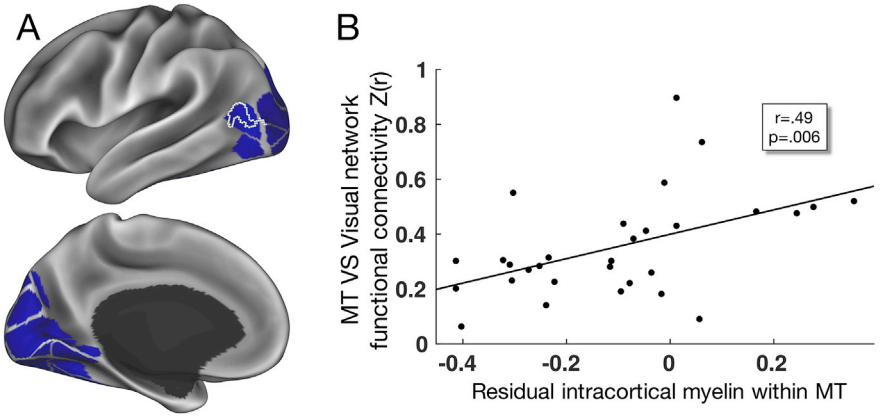

Fig. 4. Intracortical myelin in the MT+ region is associated with Visual network functional connectivity. A) The TBI-influenced region (white outline) corresponds well with an a priori parcel (from Gordon et al., 2016) in the Visual network (blue regions). B) The strength of the intracortical myelin contrast within the putative MT+ region (x-axis) was positively associated with the strength of functional connectivity between this region and the Visual network parcels (y-axis).

injuries that cannot be detected using diffusion imaging. Importantly, as interneuron function—and particularly the balance between excitatory and inhibitory interneuron signaling—is critical for optimal cortical processing (Maffei et al., 2006; Marín, 2012; Yizhar et al., 2011), demyelination/damage within cortex could in principle influence cortical function as much or more than deep white demyelination.

Effects of TBI on cortical myelin were strongest in the lateral occipital cortex, and in this region the TBI-myelin relationship survived a stringent permutation-based cluster correction for multiple comparisons. Importantly, this specific region with a significant TBI-myelin relationship overlapped strikingly with the known location of a highly myelinated region in lateral occipital cortex that has been argued to represent the human MT+ complex, a well-studied visual processing area (Clarke and Miklossy, 1990; Glasser and Van Essen, 2011; Tootell and Taylor, 1995). This finding suggests that TBIs may have particularly strong impacts on the myelinated structure of the visual processing area MT.

In support of this idea, we further found that intracortical myelin in this region was associated with the strength of functional connectivity to the network of regions supporting visual processing, but not to other brain networks. This suggests that TBI-related demyelination of cortex also affects the visual-related functions of area MT. As area MT is believed to be critical for visual processing of motion and subsequent directing of eye movements (Born and Bradley, 2005; Dubner and Zeki, 1971), the MT-specific myelin loss and subsequent impaired network connectivity with other visual processing regions that we observe here could partly underlie the robust findings of TBI-related deficits in oculomotor functions such as saccades and smooth visual pursuit (Hunt et al., 2016; Mani et al., 2018)—a possibility which should be investigated in future work.

Although we focus here on the MT region, we do not claim that this is the only area in which intracortical myelin is affected by TBI. TBI-related deficits in cognition can be extensive and, aside from oculomotor deficits, often manifest in impaired executive function and emotion regulation (Agoston and Kamnaksh, 2015; Cole and Bailie, 2016), functions which are dependent on widespread regions in lateral and medial prefrontal and parietal cortex. Similarly, effects of TBI on diffusion MRI measures are often characterized as being widespread and diffuse (Davenport et al., 2012; Hayes et al., 2015; Ware et al., 2017). While the MT region was the only one that survived stringent statistical significance thresholding in this work (Fig. 3), many other regions did exhibit widespread but moderate negative relationships between TBI and the myelin contrast signal, including lateral and medial prefrontal and parietal cortex (Fig. 2). We hypothesize that, as a highly-myelinated region, MT may simply have more baseline myelin to be lost, and so TBI-related injuries to this section of cortex may be more detectable via myelin mapping than injuries to association cortex.

Overall, it is of high interest to identify mechanistic links between TBIs, structural brain damage, alterations in brain function, and cognitive/behavioral deficits and symptoms. Such links have been difficult to establish using diffusion imaging, possibly because diffusion imaging-derived white matter integrity does not consistently correlate with brain function, as typically measured using fMRI (Gordon et al., 2018; Hirsiger et al., 2016; Tsang et al., 2017). This lack of correspondence between diffusion and fMRI measures may be because the fMRI BOLD signal is known to correspond primarily to local interneuron activity rather than to pyramidal spiking activity (Goense and Logothetis, 2008; Logothetis et al., 2001). Importantly, the measures of intracortical myelin we obtained here likely contain more information about the integrity of local cortical interneurons than diffusion imaging can provide, and so may be easier to link to measures of brain function. This idea is supported by our finding that TBI-affected measures of intracortical myelin in area MT were associated with functional network connectivity. As such, we hypothesize that myelin mapping may be more generally useful for establishing injury-structure-function-behavior links than diffusion imaging. This hypothesis should be tested in future work employing data collection in all three modalities (fMRI, DTI, and myelin).

A major goal of studying TBI using neuroimaging measures is ultimately to employ these techniques for the diagnosis of TBI and/or the prognosis of symptoms and cognitive deficits that may persist or emerge, given a particular patient's injury. Diffusion imaging alone, while sensitive to TBI presence (Asken et al., 2018; Douglas et al., 2015; Fox et al., 2013; Hulkower et al., 2013; Kaplan et al., 2018; Niogi and Mukherjee, 2010; Sharp and Ham, 2011; Shenton et al., 2012; Strauss et al., 2015) and statistically predictive of cognitive/behavioral outcomes (van Eijck et al., 2018; Gordon et al., 2018; Gu et al., 2013; Kraus et al., 2007; Kumar et al., 2009; Matsushita et al., 2011; Palacios et al., 2011; Roberts et al., 2016; Wada et al., 2012; Wallace et al., 2018b; Xiong et al., 2014), does not appear to have the sensitivity needed for reliable diagnosis or prognosis in individual patients (Douglas et al., 2015; Mac Donald et al., 2011). In this work we found that neuroimaging-based measures of intracortical myelin—which, in indexing the integrity of cortical rather than deep white axons, are complementary to diffusion measures—are also sensitive to TBI and associated with brain function. It is thus possible that diagnostic sensitivity could be increased by combining these complementary diffusion and myelin mapping measures, though future work is needed to determine exactly how best to combine the two measures to optimize sensitivity and specificity.

Perhaps surprisingly, we found that blast injury did not induce intracortical myelin changes that could be differentiated from those caused by blunt-force trauma. In contrast, diffusion imaging has demonstrated that blast injuries reduce the integrity of deep white matter tracts to a greater extent than blunt-force trauma (Davenport et al., 2012; Taber et al., 2015). Blast effects may thus be a domain in which the intracortical myelin signal is less sensitive to injury than diffusion imaging, which may underscore the need to use these techniques in a complementary fashion in future work in order to establish maximally predictive prognostic models.

4.1. Limitations

The evaluation of TBI conducted here was based on self-report, which is an unavoidable limitation when assessing lifetime TBI histories. As TBIs impact the fidelity of memories surrounding the event, some inaccuracy in these self-report histories is expected, which may be a major reason why associations between the lifetime number of TBIs and intracortical myelin were weaker than associations between intracortical myelin and functional connectivity. This work also examined patients often many years after their TBI occurred, which is a significant limitation, as we could not examine how intracortical myelin might be affected proximal to the injury. Future work could longitudinally track TBI patients after well-documented injuries in order to determine how specifically intracortical myelin is affected, as well as the post-injury timeline of effects.

The T1-w/T2-w ratio map strongly resembles the known distribution of cortical myelin in this work (Fig. 1) and in previous work (Glasser and Van Essen, 2011). This suggests that myelination is the primary cause of spatial variation in this signal in healthy and in TBI-affected brains. However, this signal is certainly not a pure probe for myelin, but may also be affected in local regions by specific injury-related factors that are known to affect the T1-w and/or T2-w signals such as inflammation (Michoux et al., 2015), or invasion of CSF into the intracortical space. Therefore, while we consider reductions in intracortical myelination to be the most likely driver of the observed relationships between lifetime TBIs and the T1-w/T2-w ratio, future work is needed to establish the degree to which other factors may also be contributing.

5. Conclusion

Here we demonstrated for the first time that intracortical myelin, as measured using the T1-w/T2 ratio method of myelin mapping, is sensitive to TBI, and that TBI-related disruption of intracortical myelin affects brain function. This finding suggests that intracortical myelin may be

useful as a biomarker of TBI. As intracortical myelin is anatomically complementary to diffusion-based measures of deep white matter, future work should explore whether measures of intracortical myelin may usefully be combined with diffusion imaging and functional imaging measures to improve the sensitivity and specificity of MRI-based diagnostic tools for TBI. Development of such diagnostic tools may in turn improve prognoses of a patient's expected level of long-term TBI-related deficit.

Funding

This work was supported by Career Development Award #1IK2CX001680 from the US Department of Veterans Affairs Clinical Sciences Research and Development Service, and by VA VISN17 Center of Excellence pilot funding. The contents of this manuscript do not represent the views of the US Department of Veterans Affairs or the United States Government.

Acknowledgments

The authors thank Ramy Sweidan, Brad Gary, Staley Justice, Leslie Danhaus, Habib Abla, Krupa George, Janani Srikanth, Allison McGinnis, and Robert Athey for their assistance in data collection and behavioral data coding.

Appendix A. Supplementary data

Supplementary data to this article can be found online at https://doi.org/10.1016/j.neuroimage.2019.06.026.

References

Agoston, D.V., Kamnaksh, A., 2015. Modeling the neurobehavioral consequences of blast-induced traumatic brain injury spectrum disorder and identifying related biomarkers. In: Kobeissy, F.H. (Ed.), Brain Neurotrauma: Molecular, Neuropsychological, and Rehabilitation Aspects. CRC Press/Taylor & Francis, Boca Raton (FL.

Asken, B.M., DeKosky, S.T., Clugston, J.R., Jaffee, M.S., Bauer, R.M., 2018. Diffusion tensor imaging (DTI) findings in adult civilian, military, and sport-related mild traumatic brain injury (mTBI): a systematic critical review. Brain Imaging Behav 12, 585–612.

Bass, C.R., Panzer, M.B., Rafaels, K.A., Wood, G., Shridharani, J., Capehart, B., 2012. Brain injuries from blast. Ann. Biomed. Eng. 40, 185–202.

Belanger, H.G., Curtiss, G., Demery, J.A., Lebowitz, B.K., Vanderploeg, R.D., 2005. Factors moderating neuropsychological outcomes following mild traumatic brain injury: a meta-analysis. J. Int. Neuropsychol. Soc. JINS 11, 215–227.

Bharath, R.D., Munivenkatappa, A., Gohel, S., Panda, R., Saini, J., Rajeswaran, J., Shukla, D., Bhagavatula, I.D., Biswal, B.B., 2015. Recovery of resting brain connectivity ensuing mild traumatic brain injury. Front. Hum. Neurosci. 9, 513.

Born, R.T., Bradley, D.C., 2005. Structure and function of visual area mt. Annu. Rev. Neurosci. 28, 157–189.

Bruce, M.L., 2010. Suicide risk and prevention in veteran populations. Ann. N. Y. Acad. Sci. 1208, 98–103.

Cappa, K.A., Conger, J.C., Conger, A.J., 2011. Injury severity and outcome: a meta-analysis of prospective studies on TBI outcome. Health Psychol. Off. J. Div. Health Psychol. Am. Psychol. Assoc. 30, 542–560.

Carp, J., 2013. Optimizing the order of operations for movement scrubbing: comment on Power et al. Neuroimage 76, 436–438.

Chien, D.-K., Hwang, H.-F., Lin, M.-R., 2017. Injury severity measures for predicting return-to-work after a traumatic brain injury. Accid. Anal. Prev. 98, 101–107.

Ciric, R., Wolf, D.H., Power, J.D., Roalf, D.R., Baum, G., Ruparel, K., Shinohara, R.T., Elliott, M.A., Eickhoff, S.B., Davatzikos, C., et al., 2017. Benchmarking of participant-level confound regression strategies for the control of motion artifact in studies of functional connectivity. Neuroimage 154, 174–187.

Clarke, S., Miklossy, J., 1990. Occipital cortex in man: organization of callosal connections, related myelo- and cytoarchitecture, and putative boundaries of functional visual areas. J. Comp. Neurol. 298, 188–214.

Cole, W.R., Bailie, J.M., 2016. Neurocognitive and psychiatric symptoms following mild traumatic brain injury. In: Laskowitz, D., Grant, G. (Eds.), Translational Research in Traumatic Brain Injury. CRC Press/Taylor and Francis Group, Boca Raton (FL.

Corrigan, J.D., Bogner, J., 2007. Initial reliability and validity of the Ohio state university TBI identification method. J. Head Trauma Rehabil. 22, 318–329.

Dale, A.M., Sereno, M.I., 1993. Improved localizadon of cortical activity by combining EEG and MEG with MRI cortical surface reconstruction: a linear approach. J. Cogn. Neurosci. 5, 162–176.

Dale, A.M., Fischl, B., Sereno, M.I., 1999. Cortical surface-based analysis: I. Segmentation and surface reconstruction. Neuroimage 9, 179–194.

Davceva, N., Janevska, V., Ilievski, B., Petrushevska, G., Popeska, Z., 2012. The occurrence of acute subdural haematoma and diffuse axonal injury as two typical acceleration injuries. J. Forensic Leg. Med. 19, 480–484.

Davenport, N.D., Lim, K.O., Armstrong, M.T., Sponheim, S.R., 2012. Diffuse and spatially variable white matter disruptions are associated with blast-related mild traumatic brain injury. Neuroimage 59, 2017–2024.

Dikmen, S., Machamer, J., Temkin, N., 2001. Mild head injury: facts and artifacts. J. Clin. Exp. Neuropsychol. 23, 729–738.

Douglas, D.B., Iv, M., Douglas, P.K., Anderson, A., Vos, S.B., Bammer, R., Zeineh, M., Wintermark, M., 2015. Diffusion tensor imaging of TBI: potentials and challenges. Top. Magn. Reson. Imag. 24, 241.

Dubner, R., Zeki, S.M., 1971. Response properties and receptive fields of cells in an anatomically defined region of the superior temporal sulcus in the monkey. Brain Res. 35, 528–532.

Eklund, A., Nichols, T.E., Knutsson, H., 2016. Cluster failure: why fMRI inferences for spatial extent have inflated false-positive rates. Proc. Natl. Acad. Sci. Unit. States Am. 113, 7900–7905.

Elsayed, N.M., 1997. Toxicology of blast overpressure. Toxicology 121, 1–15.

Fair, D.A., Miranda-Dominguez, O., Snyder, A.Z., Perrone, A.A., Earl, E.A., Van, A.N., Koller, J.M., Feczko, E., Klein, R.L., Mirro, A.E., et al., 2018. Correction of respiratory artifacts in MRI head motion estimates. BioRxiv 337360.

Fischl, B., Sereno, M.I., Dale, A.M., 1999. Cortical surface-based analysis: II: inflation, flattening, and a surface-based coordinate system. Neuroimage 9, 195–207.

Fox, W.C., Park, M.S., Belverud, S., Klugh, A., Rivet, D., Tomlin, J.M., 2013. Contemporary imaging of mild TBI: the journey toward diffusion tensor imaging to assess neuronal damage. Neurol. Res. 35, 223–232.

Friston, K.J., Williams, S., Howard, R., Frackowiak, R.S.J., Turner, R., 1996. Movement-Related effects in fMRI time-series. Magn. Reson. Med. 35, 346–355.

Ganpule, S., Alai, A., Plougonven, E., Chandra, N., 2013. Mechanics of blast loading on the head models in the study of traumatic brain injury using experimental and computational approaches. Biomechanics Model. Mechanobiol. 12, 511–531.

Ganzetti, M., Wenderoth, N., Mantini, D., 2014. Whole brain myelin mapping using T1- and T2-weighted MR imaging data. Front. Hum. Neurosci. 8, 671.

Glasser, M.F., Van Essen, D.C., 2011. Mapping human cortical areas in vivo based on myelin content as revealed by T1- and T2-weighted MRI. J. Neurosci. 31, 11597–11616.

Glasser, M.F., Sotiropoulos, S.N., Wilson, J.A., Coalson, T.S., Fischl, B., Andersson, J.L., Xu, J., Jbabdi, S., Webster, M., Polimeni, J.R., et al., 2013. The minimal preprocessing pipelines for the Human Connectome project. Neuroimage 80, 105–124.

Glasser, M.F., Coalson, T.S., Robinson, E.C., Hacker, C.D., Harwell, J., Yacoub, E., Ugurbil, K., Andersson, J., Beckmann, C.F., Jenkinson, M., et al., 2016. A multi-modal parcellation of human cerebral cortex. Nature 536, 171–178.

Goense, J.B.M., Logothetis, N.K., 2008. Neurophysiology of the BOLD fMRI signal in awake monkeys. Curr. Biol. 18, 631–640.

Gordon, E.M., Laumann, T.O., Adeyemo, B., Huckins, J.F., Kelley, W.M., Petersen, S.E., 2016. Generation and evaluation of a cortical area parcellation from resting-state correlations. Cerebr. Cortex 26, 288–303.

Gordon, E.M., Laumann, T.O., Gilmore, A.W., Newbold, D.J., Greene, D.J., Berg, J.J., Ortega, M., Hoyt-Drazen, C., Gratton, C., Sun, H., et al., 2017a. Precision functional mapping of individual human brains. Neuron 95, 791–807.

Gordon, E.M., Laumann, T.O., Adeyemo, B., Petersen, S.E., 2017b. Individual variability of the system-level organization of the human brain. Cerebr. Cortex 27, 386–399.

Gordon, E.M., Scheibel, R., Zambrano-Vazquez, L., Jia-Richards, M., May, G.J., Meyer, E.C., Nelson, S.M., 2018. High-fidelity measures of whole-brain functional connectivity and white matter integrity mediate relationships between TBI and PTSD symptoms. J. Neurotrauma 35, 767–779.

Greve, D.N., Fischl, B., 2009. Accurate and robust brain image alignment using boundary-based registration. Neuroimage 48, 63–72.

Grydeland, H., Walhovd, K.B., Tamnes, C.K., Westlye, L.T., Fjell, A.M., 2013. Intracortical myelin links with performance variability across the human lifespan: results from T1- and T2-weighted MRI myelin mapping and diffusion tensor imaging. J. Neurosci. 33, 18618–18630.

Grydeland, H., Westlye, L.T., Walhovd, K.B., Fjell, A.M., 2016. Intracortical posterior cingulate myelin content relates to error processing: results from T1- and T2-weighted MRI myelin mapping and electrophysiology in healthy adults. Cereb. Cortex N. Y. N 26, 2402–2410, 1991.

Gu, L., Li, J., Feng, D.-F., Cheng, E.-T., Li, D.-C., Yang, X.-Q., Wang, B.-C., 2013. Detection of white matter lesions in the acute stage of diffuse axonal injury predicts long-term cognitive impairments: a clinical diffusion tensor imaging study. J. Trauma Acute Care Surg. 74, 242–247.

Hayes, J.P., Miller, D.R., Lafleche, G., Salat, D.H., Verfaellie, M., 2015. The nature of white matter abnormalities in blast-related mild traumatic brain injury. NeuroImage Clin 8, 148–156.

Hayes, J.P., Bigler, E.D., Verfaellie, M., 2016. Traumatic brain injury as a disorder of brain connectivity. J. Int. Neuropsychol. Soc. JINS 22, 120–137.

Heidemann, R.M., Anwander, A., Feiweier, T., Knösche, T.R., Turner, R., 2012. k-space and q-space: combining ultra-high spatial and angular resolution in diffusion imaging using ZOOPPA at 7T. Neuroimage 60, 967–978.

Hessen, E., Nestvold, K., Anderson, V., 2007. Neuropsychological function 23 years after mild traumatic brain injury: a comparison of outcome after paediatric and adult head injuries. Brain Inj. 21, 963–979.

Hiekkanen, H., Kurki, T., Brandstack, N., Kairisto, V., Tenovuo, O., 2009. Association of injury severity, MRI-results and ApoE genotype with 1-year outcome in mainly mild TBI: a preliminary study. Brain Inj. 23, 396–402.

Hirsiger, S., Koppelmans, V., Mérillat, S., Liem, F., Erdeniz, B., Seidler, R.D., Jäncke, L., 2016. Structural and functional connectivity in healthy aging: associations for cognition and motor behavior. Hum. Brain Mapp. 37, 855–867.
Hopf, A., 1951. Die myeloarchitektonik des isocortex temporalis beim menschen. J. Hirnforsch. 1, 208–179.
Huisman, T.A.G.M., Schwamm, L.H., Schaefer, P.W., Koroshetz, W.J., Shetty-Alva, N., Ozsunar, Y., Wu, O., Sorensen, A.G., 2004. Diffusion tensor imaging as potential biomarker of white matter injury in diffuse axonal injury. Am. J. Neuroradiol. 25, 370–376.
Hulkower, M.B., Poliak, D.B., Rosenbaum, S.B., Zimmerman, M.E., Lipton, M.L., 2013. A decade of DTI in traumatic brain injury: 10 years and 100 articles later. AJNR Am. J. Neuroradiol. 34, 2064–2074.
Hunt, A.W., Mah, K., Reed, N., Engel, L., Keightley, M., 2016. Oculomotor-based vision assessment in mild traumatic brain injury: a systematic review. J. Head Trauma Rehabil. 31, 252–261.
Iwatani, J., Ishida, T., Donishi, T., Ukai, S., Shinosaki, K., Terada, M., Kaneoke, Y., 2015. Use of T1-weighted/T2-weighted magnetic resonance ratio images to elucidate changes in the schizophrenic brain. Brain Behav 5, e00399.
Jenkinson, M., Beckmann, C.F., Behrens, T.E.J., Woolrich, M.W., Smith, S.M., 2012. FSL. NeuroImage 62, 782–790.
Jorge, R.E., Acion, L., White, T., Tordesillas-Gutierrez, D., Pierson, R., Crespo-Facorro, B., Magnotta, V.A., 2012. White matter abnormalities in veterans with mild traumatic brain injury. Am. J. Psychiatry 169, 1284–1291.
Kaplan, G.B., Leite-Morris, K.A., Wang, L., Rumbika, K.K., Heinrichs, S.C., Zeng, X., Wu, L., Arena, D.T., Teng, Y.D., 2018. Pathophysiological bases of comorbidity: TBI and PTSD. J. Neurotrauma 35, 210–225.
Kennedy, J.E., Cullen, M.A., Amador, R.R., Huey, J.C., Leal, F.O., 2010. Symptoms in military service members after blast mTBI with and without associated injuries. NeuroRehabilitation 26, 191–197.
Kraus, M.F., Susmaras, T., Caughlin, B.P., Walker, C.J., Sweeney, J.A., Little, D.M., 2007. White matter integrity and cognition in chronic traumatic brain injury: a diffusion tensor imaging study. Brain 130, 2508–2519.
Kumar, R., Gupta, D.R.K., Husain, M., Chaudhry, C., Srivastava, A., Saksena, S., Rathore, R.K.S., 2009. Comparative evaluation of corpus callosum DTI metrics in acute mild and moderate traumatic brain injury: its correlation with neuropsychometric tests. Brain Inj. 23, 675–685.
Langlois, J.A., Rutland-Brown, W., Wald, M.M., 2006. The epidemiology and impact of traumatic brain injury: a brief overview. J. Head Trauma Rehabil. 21, 375–378.
Logothetis, N.K., Pauls, J., Augath, M., Trinath, T., Oeltermann, A., 2001. Neurophysiological investigation of the basis of the fMRI signal. Nature 412, 150–157.
Mac Donald, C.L., Johnson, A.M., Cooper, D., Nelson, E.C., Werner, N.J., Shimony, J.S., Snyder, A.Z., Raichle, M.E., Witherow, J.R., Fang, R., et al., 2011. Detection of blast-related traumatic brain injury in U.S. military personnel. N. Engl. J. Med. 364, 2091–2100.
Maffei, A., Nataraj, K., Nelson, S.B., Turrigiano, G.G., 2006. Potentiation of cortical inhibition by visual deprivation. Nature 443, 81–84.
Mani, R., Asper, L., Khuu, S.K., 2018. Deficits in saccades and smooth-pursuit eye movements in adults with traumatic brain injury: a systematic review and meta-analysis. Brain Inj. 32, 1315–1336.
Marcus, D., Harwell, J., Olsen, T., Hodge, M., Glasser, M., Prior, F., Jenkinson, M., Laumann, T., Curtiss, S., Van Essen, D., 2011. Informatics and data mining tools and strategies for the human connectome project. Front. Neuroinf. 5.
Marek, S., Siegel, J.S., Gordon, E.M., Raut, R.V., Gratton, C., Newbold, D.J., Ortega, M., Laumann, T.O., Adeyemo, B., Miller, D.B., et al., 2018. Spatial and temporal organization of the individual human cerebellum. Neuron 100, 977–993.
Marín, O., 2012. Interneuron dysfunction in psychiatric disorders. Nat. Rev. Neurosci. 13, 107–120.
Matsushita, M., Hosoda, K., Naitoh, Y., Yamashita, H., Kohmura, E., 2011. Utility of diffusion tensor imaging in the acute stage of mild to moderate traumatic brain injury for detecting white matter lesions and predicting long-term cognitive function in adults: clinical article. J. Neurosurg. 115, 130–139.
McNab, J.A., Polimeni, J.R., Wang, R., Augustinack, J.C., Fujimoto, K., Stevens, A., Janssens, T., Farivar, R., Folkerth, R.D., Vanduffel, W., et al., 2013. Surface based analysis of diffusion orientation for identifying architectonic domains in the in vivo human cortex. Neuroimage 69, 87–100.
Michoux, N., Guillet, A., Rommel, D., Mazzamuto, G., Sindic, C., Duprez, T., 2015. Texture analysis of T2-weighted MR images to assess acute inflammation in brain MS lesions. PLoS One 10, e0145497.
Moore, D.F., Jaffee, M.S., 2010. Military traumatic brain injury and blast. NeuroRehabilitation 26, 179–181.
Nieuwenhuys, R., 2013. The myeloarchitectonic studies on the human cerebral cortex of the Vogt-Vogt school, and their significance for the interpretation of functional neuroimaging data. In: Microstructural Parcellation of the Human Cerebral Cortex. Springer, Berlin, Heidelberg, pp. 55–125.
Nieuwenhuys, R., Broere, C.A.J., 2017. A map of the human neocortex showing the estimated overall myelin content of the individual architectonic areas based on the studies of Adolf Hopf. Brain Struct. Funct. 222, 465–480.
Niogi, S.N., Mukherjee, P., 2010. Diffusion tensor imaging of mild traumatic brain injury. J. Head Trauma Rehabil. 25, 241–255.
Palacios, E.M., Fernandez-Espejo, D., Junque, C., Sanchez-Carrion, R., Roig, T., Tormos, J.M., Bargallo, N., Vendrell, P., 2011. Diffusion tensor imaging differences relate to memory deficits in diffuse traumatic brain injury. BMC Neurol. 11, 24.
Palomero-Gallagher, N., Zilles, K., 2017. Cortical layers: cyto-, myelo-, receptor- and synaptic architecture in human cortical areas. NeuroImage. https://doi.org/10.1016/j.neuroimage.2017.08.035. Advance Access.
Pearce, J.M.S., 2008. Observations on concussion. Eur. Neurol. 59, 113–119.
Power, J.D., Barnes, K.A., Snyder, A.Z., Schlaggar, B.L., Petersen, S.E., 2012. Spurious but systematic correlations in functional connectivity MRI networks arise from subject motion. Neuroimage 59, 2142–2154.
Power, J.D., Mitra, A., Laumann, T.O., Snyder, A.Z., Schlaggar, B.L., Petersen, S.E., 2014. Methods to detect, characterize, and remove motion artifact in resting state fMRI. Neuroimage 84, 320–341.
Rathi, Y., Pasternak, O., Savadjiev, P., Michailovich, O., Bouix, S., Kubicki, M., Westin, C.-F., Makris, N., Shenton, M.E., 2014. Gray matter alterations in early aging: a diffusion magnetic resonance imaging study. Hum. Brain Mapp. 35, 3841–3856.
Righart, R., Biberacher, V., Jonkman, L.E., Klaver, R., Schmidt, P., Buck, D., Berthele, A., Kirschke, J.S., Zimmer, C., Hemmer, B., et al., 2017. Cortical pathology in multiple sclerosis detected by the T1/T2-weighted ratio from routine magnetic resonance imaging. Ann. Neurol. 82, 519–529.
Roberts, R.M., Mathias, J.L., Rose, S.E., 2016. Relationship between diffusion tensor imaging (DTI) findings and cognition following pediatric TBI: a meta-analytic review. Dev. Neuropsychol. 41, 176–200.
Rohling, M.L., Demakis, G.J., 2010. Bowden, shores, & Mathias (2006): failure to replicate or just failure to notice. Does effort still account for more variance in neuropsychological test scores than TBI severity? Clin. Neuropsychol. 24, 119–136.
Rosenfeld, J.V., Ford, N.L., 2010. Bomb blast, mild traumatic brain injury and psychiatric morbidity: a review. Injury 41, 437–443.
Rutgers, D.R., Fillard, P., Paradot, G., Tadié, M., Lasjaunias, P., Ducreux, D., 2008a. Diffusion tensor imaging characteristics of the corpus callosum in mild, moderate, and severe traumatic brain injury. Am. J. Neuroradiol. 29, 1730–1735.
Rutgers, D.R., Toulgoat, F., Cazejust, J., Fillard, P., Lasjaunias, P., Ducreux, D., 2008b. White matter abnormalities in mild traumatic brain injury: a diffusion tensor imaging study. Am. J. Neuroradiol. 29, 514–519.
Ségonne, F., Dale, A.M., Busa, E., Glessner, M., Salat, D., Hahn, H.K., Fischl, B., 2004. A hybrid approach to the skull stripping problem in MRI. Neuroimage 22, 1060–1075.
Ségonne, F., Grimson, E., Fischl, B., 2005. A genetic algorithm for the topology correction of cortical surfaces. In: Christensen, G.E., Sonka, M. (Eds.), Information Processing in Medical Imaging. Glenwood Springs, CO, USA, p. 393. Springer.
Shafee, R., Buckner, R.L., Fischl, B., 2015. Gray matter myelination of 1555 human brains using partial volume corrected MRI images. Neuroimage 105, 473–485.
Sharp, D.J., Ham, T.E., 2011. Investigating white matter injury after mild traumatic brain injury. Curr. Opin. Neurol. 24, 558–563.
Shenton, M.E., Hamoda, H.M., Schneiderman, J.S., Bouix, S., Pasternak, O., Rathi, Y., Vu, M.-A., Purohit, M.P., Helmer, K., Koerte, I., et al., 2012. A review of magnetic resonance imaging and diffusion tensor imaging findings in mild traumatic brain injury. Brain Imaging Behav 6, 137–192.
Shi, H., Hu, X., Leak, R.K., Shi, Y., An, C., Suenaga, J., Chen, J., Gao, Y., 2015. Demyelination as a rational therapeutic target for ischemic or traumatic brain injury. Exp. Neurol. 272, 17–25.
Sigalovsky, I.S., Fischl, B., Melcher, J.R., 2006. Mapping an intrinsic MR property of gray matter in auditory cortex of living humans: a possible marker for primary cortex and hemispheric differences. Neuroimage 32, 1524–1537.
Silver, J.M., McAllister, T.W., Yudofsky, S.C., 2011. Textbook of Traumatic Brain Injury. American Psychiatric Publishing, Arlington, VA.
Song, A.W., Chang, H.-C., Petty, C., Guidon, A., Chen, N.-K., 2014. Improved delineation of short cortical association fibers and gray/white matter boundary using whole-brain three-dimensional diffusion tensor imaging at submillimeter spatial resolution. Brain Connect. 4, 636–640.
Stevens, M.C., Lovejoy, D., Kim, J., Oakes, H., Kureshi, I., Witt, S.T., 2012. Multiple resting state network functional connectivity abnormalities in mild traumatic brain injury. Brain Imaging Behav 6, 293–318.
Strauss, S., Hulkower, M., Gulko, E., Zampolin, R.L., Gutman, D., Chitkara, M., Zughaft, M., Lipton, M.L., 2015. Current clinical applications and future potential of diffusion tensor imaging in traumatic brain injury. Top. Magn. Reson. Imaging TMRI 24, 353–362.
Taber, K.H., Hurley, R.A., Haswell, C.C., Rowland, J.A., Hurt, S.D., Lamar, C.D., Morey, R.A., 2015. White matter compromise in veterans exposed to primary blast forces. J. Head Trauma Rehabil. 30, E15–E25.
Taylor, C.A., Bell, J., Breiding, M., Xu, L., 2017. Traumatic brain injury–related emergency department visits, hospitalizations, and deaths — United States, 2007 and 2013. MMWR Surveill. Summ. 66, 1–16.
Thompson, J.M., Scott, K.C., Dubinsky, L., 2008. Battlefield brain: unexplained symptoms and blast-related mild traumatic brain injury. Can. Fam. Physician Médecin Fam. Can. 54, 1549–1551.
Tootell, R.B.H., Taylor, J.B., 1995. Anatomical evidence for MT and additional cortical visual areas in humans. Cerebr. Cortex 5, 39–55.
Tsang, A., Lebel, C.A., Bray, S.L., Goodyear, B.G., Hafeez, M., Sotero, R.C., McCreary, C.R., Frayne, R., 2017. White matter structural connectivity is not correlated to cortical resting-state functional connectivity over the healthy adult lifespan. Front. Aging Neurosci. 9, 144.
Ursano, R.J., Goldenberg, M., Zhang, L., Carlton, J., Fullerton, C.S., Li, H., Johnson, L., Benedek, D., 2010. Posttraumatic stress disorder and traumatic stress: from bench to bedside, from war to disaster. Ann. N. Y. Acad. Sci. 1208, 72–81.
Vakhtin, A.A., Calhoun, V.D., Jung, R.E., Prestopnik, J.L., Taylor, P.A., Ford, C.C., 2013. Changes in intrinsic functional brain networks following blast-induced mild traumatic brain injury. Brain Inj. 27, 1304–1310.
van Eijck, M.M., Schoonman, G.G., van der Naalt, J., de Vries, J., Roks, G., 2018. Diffuse axonal injury after traumatic brain injury is a prognostic factor for functional outcome: a systematic review and meta-analysis. Brain Inj. 32, 395–402.

Van Essen, DavidC., Drury, H.A., Dickson, J., Harwell, J., Hanlon, D., Anderson, C.H., 2001. An integrated software suite for surface-based analyses of cerebral cortex. J. Am. Med. Inform. Assoc. 8, 443–459.
Van Essen, D.C., Glasser, M.F., Dierker, D.L., Harwell, J., Coalson, T., 2012. Parcellations and hemispheric asymmetries of human cerebral cortex analyzed on surface-based atlases. Cerebr. Cortex 22, 2241–2262.
Vanderploeg, R.D., Curtiss, G., Luis, C.A., Salazar, A.M., 2007. Long-term morbidities following self-reported mild traumatic brain injury. J. Clin. Exp. Neuropsychol. 29, 585–598.
Vanderploeg, R.D., Belanger, H.G., Curtiss, G., 2009. Mild traumatic brain injury and posttraumatic stress disorder and their associations with health symptoms. Arch. Phys. Med. Rehabil. 90, 1084–1093.
Vasterling, J.J., Schumm, J., Proctor, S.P., Gentry, E., King, D.W., King, L.A., 2008. Posttraumatic stress disorder and health functioning in a non-treatment-seeking sample of Iraq war veterans: a prospective analysis. J. Rehabil. Res. Dev. 45, 347–358.
Wada, T., Asano, Y., Shinoda, J., 2012. Decreased fractional anisotropy evaluated using tract-based spatial statistics and correlated with cognitive dysfunction in patients with mild traumatic brain injury in the chronic stage. Am. J. Neuroradiol. 33, 2117–2122.
Wallace, E.J., Mathias, J.L., Ward, L., 2018a. Diffusion tensor imaging changes following mild, moderate and severe adult traumatic brain injury: a meta-analysis. Brain Imaging Behav 12, 1607–1621.
Wallace, E.J., Mathias, J.L., Ward, L., 2018b. The relationship between diffusion tensor imaging findings and cognitive outcomes following adult traumatic brain injury: a meta-analysis. Neurosci. Biobehav. Rev. 92, 93–103.
Ware, J.B., Hart, T., Whyte, J., Rabinowitz, A., Detre, J.A., Kim, J., 2017. Inter-subject variability of axonal injury in diffuse traumatic brain injury. J. Neurotrauma 34, 2243–2253.
Wojcik, B.E., Stein, C.R., Bagg, K., Humphrey, R.J., Orosco, J., 2010. Traumatic brain injury hospitalizations of U.S. Army soldiers deployed to Afghanistan and Iraq. Am. J. Prev. Med. 38, S108–S116.
Wozniak, J.R., Krach, L., Ward, E., Mueller, B.A., Muetzel, R., Schnoebelen, S., Kiragu, A., Lim, K.O., 2007. Neurocognitive and neuroimaging correlates of pediatric traumatic brain injury: a diffusion tensor imaging (DTI) study. Arch. Clin. Neuropsychol. 22, 555–568.
Xiong, K., Zhu, Y., Zhang, Y., Yin, Z., Zhang, J., Qiu, M., Zhang, W., 2014. White matter integrity and cognition in mild traumatic brain injury following motor vehicle accident. Brain Res. 1591, 86–92.
Yizhar, O., Fenno, L.E., Prigge, M., Schneider, F., Davidson, T.J., O'Shea, D.J., Sohal, V.S., Goshen, I., Finkelstein, J., Paz, J.T., et al., 2011. Neocortical excitation/inhibition balance in information processing and social dysfunction. Nature 477, 171–178.
Yoshiura, T., Higano, S., Rubio, A., Shrier, D.A., Kwok, W.E., Iwanaga, S., Numaguchi, Y., 2000. Heschl and superior temporal gyri: low signal intensity of the cortex on T2-weighted MR images of the normal brain. Radiology 214, 217–221.
Zaloshnja, E., Miller, T., Langlois, J.A., Selassie, A.W., 2008. Prevalence of long-term disability from traumatic brain injury in the civilian population of the United States, 2005. J. Head Trauma Rehabil. 23, 394–400.
Zhang, Y., Brady, M., Smith, S., 2001. Segmentation of brain MR images through a hidden Markov random field model and the expectation-maximization algorithm. IEEE Trans. Med. Imaging 20, 45–57.
Zhang, J., Yoganandan, N., Pintar, F.A., Gennarelli, T.A., 2006. Role of translational and rotational accelerations on brain strain in lateral head impact. Biomed. Sci. Instrum. 42, 501–506.